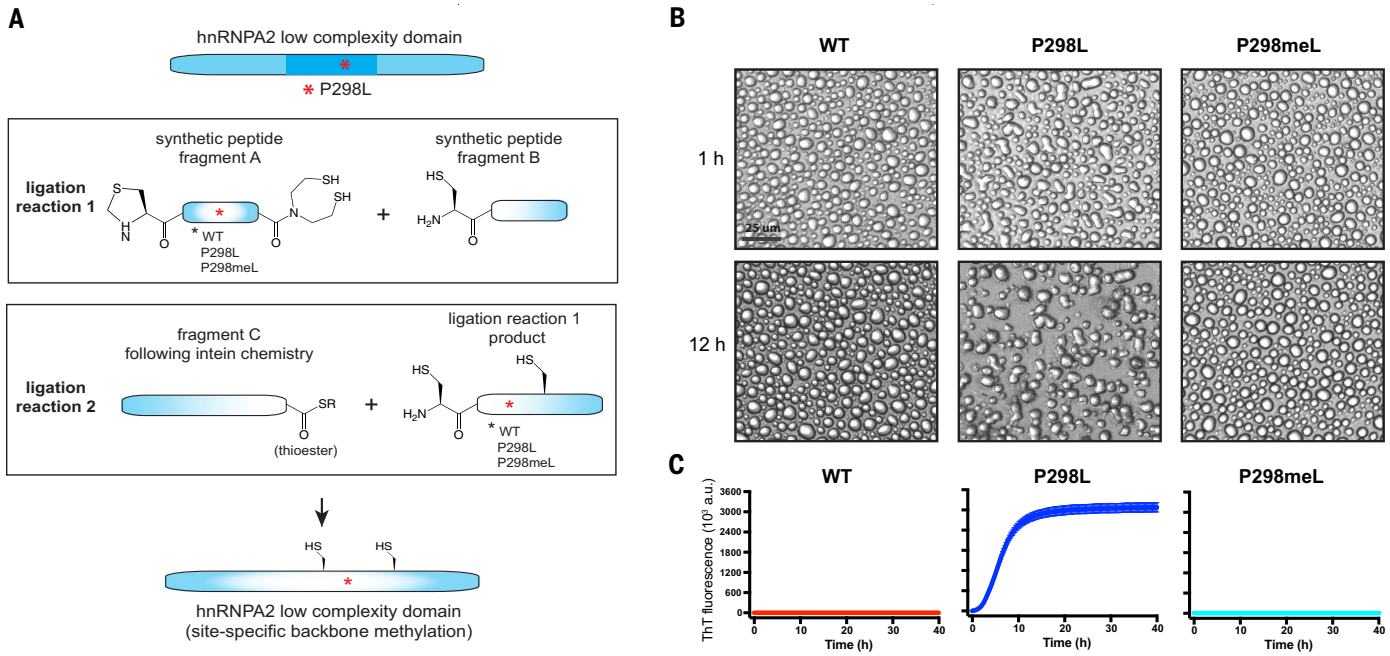

Fig. 9. Restorative effect of eliminating the main-chain hydrogen bond by methyl capping the peptide backbone nitrogen atom of the P298L mutational variant of hnRNPA2. (**A**) Top, schematic representation of the hnRNPA2 LCD with the position of the disease-causing mutant P298L (red asterisk) and self-association core region (dark blue shading) highlighted. Below is an outline of the strategy to prepare semisynthetic variants of the full-length LCD of hnRNPA2. (**B**) The assembled hnRNPA2 LCDs containing the native sequence (WT), P298L variant, and P298meL variant were tested for phase separation in an aqueous buffer. WT hnRNPA2 LCD formed spherical, liquid-like droplets (left). The P298L variant formed distinctly misshapen droplets (middle). The P298meL variant formed spherical droplets indistinguishable from those formed by the native protein (right). Scale bar, 25 µm. (**C**) Synthetic peptides used to assemble semisynthetic proteins assayed in (B) were incubated in the presence of ThT as an assay of time-dependent polymerization. No evidence of fluorescence increase was observed for WT peptide. A large, time-dependent increase in ThT fluorescence was observed for the P298L peptide, and no fluorescence increase was observed for the P298meL peptide.

cap was placed on the peptide backbone nitrogen atom of the leucine, serine, or threonine mutational variant residues. As shown in Fig. 8B, the methyl-capped derivatives of all three tau variant peptides regained solubility indistinguishable from the native tau peptide.

Moving from test tube reactions to living cells, we used a tau biosensor cell line expressing tau-CFP and tau-YFP. The fluorescent tau protein in these cells is homogeneously distributed yet can be converted to a punctate distribution when the cells are exposed to pathological tau aggregates (*54*, *55*). Each of the tau peptides studied in biochemical assays (Fig. 8B) was internalized by lipofection into the tau biosensor cell line. As shown in Fig. 8C, the native tau peptide did not affect the intracellular distribution of fluorescent tau, nor did peptide variants carrying either conformer of 4-fluroproline. Peptides corresponding to the P301L, P301S, and P301T mutations, upon introduction into the tau biosensor cells, led to aggregation of the endogenous tau protein. Finally, synthetic peptide variants of the P301L, P301S, and P301T mutants bearing a methyl cap on the leucine, serine, or threonine residue caused no detectable aggregation of endogenous tau.

Methylation of the peptide backbone nitrogen of an hnRNPA2 mutational variant restores protein function

We also examined the familial, early-onset Paget's disease mutation of residue P298 in the gene encoding hnRNPA2 (*56*). Our attention to this mutation, aside from its altering of a conserved proline residue, came from the fact that the mutation is located within an LCD long understood to self-associate in a manner leading to phase separation. Indeed, the P298L Paget's disease mutation is located in the middle of the labile cross-β core of the hnRNPA2 protein, as characterized by biochemical footprinting, solid-state NMR spectroscopy, and cryo-EM (*56*–*58*).

A three-piece native chemical ligation strategy was implemented to incorporate a synthetic peptide encompassing the site of the P298L mutation into the remainder of the hnRNPA2 LCD (Fig. 9A). Reconstruction of the native hnRNPA2 LCD yielded a protein that phase separated into spherical, liquid-like droplets. The reconstructed variant carrying the P298L mutation formed distinctly misshapen droplets, as has been observed by other investigators (*59*). Methyl capping of the variant leucine residue yielded a protein that phase separated into spherical, liquid-like droplets indistinguishable from those made by the native hnRNPA2 LCD (Fig. 9B).

To further evaluate variant-mediated enhancement of self-association of the hnRNPA2 LCD, we monitored the time-dependent acquisition of ThT fluorescence. The same 20-residue peptides used to assemble the intact LCD of hnRNPA2 assayed in Fig. 9B were incubated in the presence of ThT. Neither the peptide bearing the native sequence nor that bearing a methyl cap on the leucine residue of the P298L variant exhibited any evidence of polymerization. By contrast, the P298L peptide exhibited robust, time-dependent acquisition of ThT fluorescence (Fig. 9C).

As in the cases of the other nine mutations evaluated in this study, removing the capacity for main-chain hydrogen bonding for the leucine residue of the P298L variant fully restored properly balanced self-associative capacity to the hnRNPA2 LCD. This conclusion can be drawn from assays of both phase separation of the intact LCD (Fig. 9B) and peptide polymerization as visualized by time-dependent acquisition of ThT flourescence (Fig. 9C).